# Power Function-Weibull Composite Distribution for Modeling Lifetime Data

Chao Wang, Mengni Guan

***Abstract*—A new three-parameter distribution, referred to as the Power Function-Weibull Composite (PFWC) distribution, is introduced. This distribution features a power function density up to an unknown threshold value and a Weibull density beyond that threshold. Depending on its parameters, the PFWC distribution can exhibit decreasing, increasing, or bathtub-shaped hazard rate functions. We derive maximum likelihood, moment, and nonlinear least squares estimators for the distribution parameters. A simulation study is conducted to evaluate the performance of these estimation methods, supported by numerical computations. Additionally, tables of critical values for the Kolmogorov–Smirnov, Anderson–Darling, and Cramér–von Mises tests are provided for the PFWC distribution with unknown parameters. The power of these tests is also investigated under various scenarios. Finally, the practical utility of the PFWC distribution is demonstrated through the analysis of two real datasets.**

***Index Terms*—composite distribution, lifetime data, left-skewed, goodness-of-fit, negatively skewed, parameter estimation.**

## I. Introduction

VARIOUS parametric families of distributions are commonly used in the analysis of lifetime data. A few distributions, such as the exponential, Weibull, lognormal, log-logistic, and gamma distributions, occupy a central position among univariate distributions ([1]-[4]). However, when these distributions prove inadequate or unsuitable, alternative distributions are considered. Composite distributions are one such alternative.

In 2005, [5] proposed the lognormal-Pareto composite distribution, which combines a lognormal density up to an unknown threshold and a two-parameter Pareto density beyond that threshold. When applied to a dataset of 2492 Danish fire insurance losses, their model demonstrated a relatively good fit, outperforming several other heavy-tailed distributions, including the lognormal, Pareto, inverse Gaussian, gamma, and Weibull distributions. However, the theoretical two-component composite distribution of [5], with known mixing weights fixed and a priori, is restrictive in many practical situations. To address this limitation, [6] introduced a second lognormal-Pareto composite distribution, which assumes the mixing weight varies with distribution parameters. Using the same dataset, they showed that this modified distribution outperformed the orginal lognormal-Pareto composite distribution proposed by [5].

Since 2005, various composite distributions have been proposed in the literature, including the lognormal-Pareto ([5], [6], [13]), lognormal-generalized Pareto ([6]), exponential-Pareto ([7]), Weibull-Pareto ([8], [10]), Weibull-inverse Weibull ([9]), Weibull-Burr ([14]), and Weibull-Lomax ([15]). Most recently, [17] introduced a power function-Weibull composite distribution for insurance claims data, following the design approach of [5]. Building on the work of [6], [18] proposed a power function-lognormal composite distribution, with applications to insurance claims and family income data.

Over the past two decades, composite distributions have found increasing applications in actuarial losses ([5], [6], [11], [12], [13]), survival times ([8]), city sizes ([14]), and reliability modeling ([9]). However, few composite distributions have been applied to model lifetime data.

In this paper, we propose the Power Function-Weibull Composite (PFWC) distribution, which can be regarded as a mixture distribution with a power function below a threshold and a truncated Weibull distribution above it. The power function, being the inverse of the Pareto model, is well-suited for modeling shorter lifetimes, while the truncated Weibull distribution effectively captures longer lifetimes. Theoretically, the PFWC distribution can handle both highly positively and negatively skewed data. Positively skewed data typically consist of smaller values with higher frequencies and occasional larger values with lower frequencies, whereas negatively skewed data exhibit occasional smaller values with lower frequencies and larger values with higher frequencies. Modeling such data requires a distribution with similar skewness characteristics. Unlike existing studies, we propose fitting the logarithms of lifetimes, rather than the raw data, to the PFWC distribution. This approach provides a novel perspective for modeling lifetime data.

The remainder of this paper is organized as follows. In Section II, we express the probability density function, cumulative distribution function, quantile function, survival function, and hazard rate function of the PFWC distribution. In Section III, statistical issues of parameter estimation are investigated, and we describe a simulation study conducted to evaluate the performance of the considered estimators. A probability plot is considered in Section IV. Section V presents goodness-of-fit tests based on the Kolmogorov–Smirnov ($D$), Anderson–Darling ($A^2$), and Cramér–von Mises ($W^2$) statistics. We describe applications to two practical datasets in Section VI and provide concluding remarks in Section VII.

Manuscript received Aug 27, 2024; revised Mar 25, 2025. This research was funded by the National Social Science Fund of China (Grant No.19BTJ051), General Project of Humanities and Social Sciences of the Education Department of Henan Province (Grant No. 2025-ZDJH-420), and General Project of Humanities and Social Sciences Research by the Ministry of Education (Grant No. 24YJCZH108).

Chao Wang is a Professor in School of Mathematics and Statistics, Anyang Normal University, Anyang, 455000, China (e-mail: aynuchw@126.com).

Mengni Guan is a Lecturer in School of Mathematics and Statistics, Anyang Normal University, Anyang, 455000, China (e-mail: 07248@aynu.edu.cn).

## II. Power function-Weibull composite distribution

### A. Description of distribution

Let X be a random variable with probability density function (PDF)

$$f(x)=\begin{cases} wf_1(x), & 0<x\le\theta,\\ (1-w)\dfrac{f_2(x)}{1-F_2(\theta)}, & \theta\le x<\infty, \end{cases} \tag{1}$$

where $w$ is a mixing weight, $0<w<1$; and $f_1(x)$ and $f_2(x)$ have the respective forms of a power function distribution and Weibull distribution, i.e.,

$$f_1(x)=\frac{\alpha x^{\alpha-1}}{\theta^\alpha}, 0<x\le\theta \tag{2}$$

and

$$f_2(x)=\frac{\tau}{x}\left(\frac{x}{\psi}\right)^\tau \exp\left[-\left(\frac{x}{\psi}\right)^\tau\right], x>0. \tag{3}$$

For the power function, $\alpha>0$ is a shape parameter and $\theta>0$ is a scale parameter; for the Weibull distribution, $\psi>0$ is a scale parameter and $\tau>0$ is a shape parameter. To impose continuity and differentiability conditions on $\theta$, we have

$$f_1(\theta)=f_2(\theta), f_1^{'}(\theta)=f_2^{'}(\theta),$$

where $f_1^{'}(\theta)$ and $f_2^{'}(\theta)$ are the respective first derivatives of $f_1(x)$ and $f_2(x)$, evaluated at $\theta$. We can obtain that

$$w\frac{\alpha}{\tau}=(1-w)\left(\frac{\theta}{\psi}\right)^\tau \tag{4}$$

and

$$\frac{\alpha}{\tau}=1-\left(\frac{\theta}{\psi}\right)^\tau. \tag{5}$$

By substituting (5) in (4), we can obtain $w=1-\alpha/\tau$. This composite density can be reparameterized and rewritten as

$$f(x)=\begin{cases} w\alpha\dfrac{x^{\alpha-1}}{\theta^\alpha}, & 0<x\le\theta,\\ w\dfrac{\alpha}{x}\left(\dfrac{x}{\theta}\right)^\tau \exp\left\{-w\left[\left(\dfrac{x}{\theta}\right)^\tau-1\right]\right\}, & \theta\le x<\infty, \end{cases} \tag{6}$$

which we will refer to as the PFWC, denoted by PFWC($\alpha,\theta,\tau$). The PFWC is a distribution in three unknown parameters: $\alpha>0$, $\theta>0$, and $\tau>0$. The cumulative distribution function $F(x)$ and quantile function $Q(p)$ are, respectively, given by

$$F(x)=\begin{cases} w\left(\dfrac{x}{\theta}\right)^\alpha, & 0<x\le\theta,\\ 1-\dfrac{\alpha}{\tau}\exp\left\{-w\left[\left(\dfrac{x}{\theta}\right)^\tau-1\right]\right\}, & \theta\le x<\infty \end{cases} \tag{7}$$

and

$$Q(p)=\begin{cases} \theta\left[\dfrac{p}{w}\right]^{1/\alpha}, & 0<p\le w,\\ \theta\left\{1-\dfrac{\ln\left[(1-p)(\tau/\alpha)\right]}{w}\right\}^{1/\tau}, & w\le p<1. \end{cases} \tag{8}$$

As illustrated in Figure 1, the PDF plots for selected values of $\alpha,\theta$, and $\tau$ indicate that the PFWC distribution is highly flexible.

Figures 2 and 3 illustrate the skewness and kurtosis, respectively, of the PFWC distribution for specific ranges of $\alpha,\theta$, and $\tau$: $0<\alpha<1$ and $2<\tau<5$ in Figure 2, and $1<\alpha<5$ and $10<\tau<15$ in Figure 3. These plots reveal that the skewness and kurtosis of the PFWC distribution can vary considerably in magnitude.

### B. Survival and Hazard Rate Functions

It follows immediately from Equation (7) that the survival function of the PFWC distribution is given by $S(x;\alpha,\theta,\tau)=1-F(x;\alpha,\theta,\tau)$, i.e.,

$$S(x)=\begin{cases} 1-w\left(\dfrac{x}{\theta}\right)^\alpha, & 0<x\le\theta,\\ \dfrac{\alpha}{\tau}\exp\left\{-w\left[\left(\dfrac{x}{\theta}\right)^\tau-1\right]\right\}, & \theta\le x<\infty. \end{cases} \tag{9}$$

The corresponding hazard rate function is obtained as $H(x;\alpha,\theta,\tau)=f(x;\alpha,\theta,\tau)/S(x;\alpha,\theta,\tau)$, i.e.,

$$H(x)=\begin{cases} \left\{w\alpha\dfrac{x^{\alpha-1}}{\theta^\alpha}\right\}\Big/\left\{1-w\left(\dfrac{x}{\theta}\right)^\alpha\right\}, & 0<x\le\theta,\\ w\dfrac{\tau}{x}\left(\dfrac{x}{\theta}\right)^\tau, & \theta\le x<\infty. \end{cases} \tag{10}$$

It is difficult to analyze the shape behavior of $H(x;\alpha,\theta,\tau)$ for $0<x\le\theta$. However, it is clear that for $\tau<1$, $\lim_{x\to\infty}H(x)\to0$, and for $\tau>1$, $\lim_{x\to\infty}H(x)\to\infty$. Figure 4 shows that the PFWC can have a decreasing, increasing, or bathtub-shaped hazard rate function, depending on its parameters.

## III. Parameter Estimation

### A. Maximum Likelihood Estimation

Let $X_1,X_2,\cdots,X_n$, be a random sample from the PFWC($\alpha,\theta,\tau$) distribution. Assume the unknown parameter $\theta$ lies between the $m^{th}$ and $(m+1)^{th}$ ordered observations, i.e., $x_m\le\theta\le x_{m+1}$, where $m$ is the number of observations less than $\theta$. Given an ordered random sample $x_1\le x_2\le\cdots\le x_m\le\theta\le x_{m+1}\le\cdots\le x_n$, the likelihood function can be expressed as

$$L(\boldsymbol{x},\boldsymbol{\omega})=\frac{(1-\alpha/\tau)^n\alpha^n}{\theta^{m\alpha+(n-m)\tau}}\exp\left[(n-m)\left(1-\frac{\alpha}{\tau}\right)\right]\prod_{i=1}^m x_i^{\alpha-1}$$
$$\prod_{i=m+1}^n x_i^{\alpha-1}\exp\left[-\left(\frac{x_i}{\theta}\right)^\tau\left(1-\frac{\alpha}{\tau}\right)\right]. \tag{11}$$

The corresponding log-likelihood function is:

$$\begin{aligned}\ln L(\boldsymbol{x},\boldsymbol{\omega})&=n\ln\left(1-\frac{\alpha}{\tau}\right)+n\ln\alpha-[m\alpha+(n-m)\tau]\ln\theta\\ &+\alpha\sum_{i=1}^m\ln x_i+\tau\sum_{i=m+1}^n\ln x_i-\sum_{i=1}^n\ln x_i\\ &-\left(1-\frac{\alpha}{\tau}\right)\sum_{i=m+1}^n\left(\frac{x_i}{\theta}\right)^\tau,\end{aligned} \tag{12}$$

where $\boldsymbol{\omega}=(\alpha,\theta,\tau)^T$.

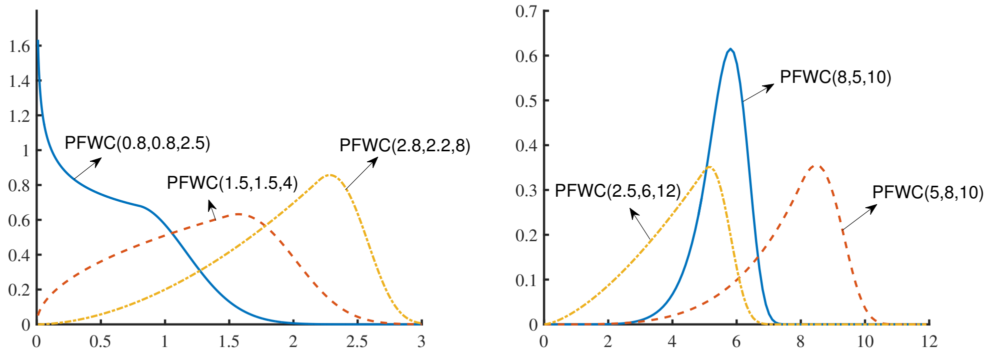


Fig 1. Plots of PFWC distribution for selected parameter values

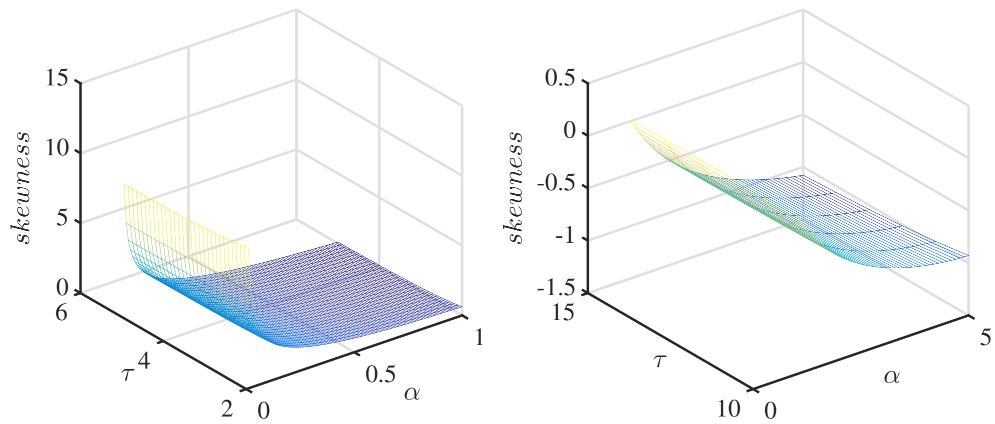


Fig 2. Plots of skewness of PFWC distribution

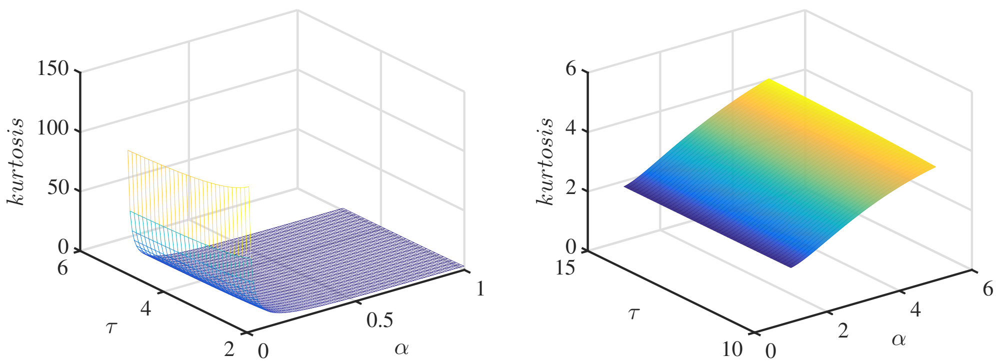


Fig 3. Plots of kurtosis of PFWC distribution

Since the maximum likelihood (ML) estimate of $\theta$ can only lie between $x_m$ and $x_{m+1}$, the ML estimators of $\omega$ can be obtained numerically through the following steps:

Step 1: For each $m = 1, 2, \cdots, n-1$, numerically find the values of $\alpha$ and $\tau$ that maximize the log-likelihood function lnL$(x, \omega)$ for $\theta$ in the interval $(x_m, x_{m+1})$. This yields $n-1$ sets of estimates:

$(\hat{\alpha}_1, \hat{\theta}_1, \hat{\tau}_1)$, $(\hat{\alpha}_2, \hat{\theta}_2, \hat{\tau}_2)$,$\cdots$, $(\hat{\alpha}_{n-1}, \hat{\theta}_{n-1}, \hat{\tau}_{n-1})$.

Step 2: Compute the log-likelihood function values for each of the $n-1$ sets of estimates. The optimal estimates, denoted by $(\hat{\alpha}_{mle}, \hat{\theta}_{mle}, \hat{\tau}_{mle})$, are those with the largest log-likelihood value among all sets.

The asymptotic variance and covariance of the ML estimators are given by the inverse of the Fisher information matrix:

$$
\begin{aligned}
\mathrm{I}(\boldsymbol{\omega}) &= -E\frac{\partial^2 \ln L(\boldsymbol{x}, \boldsymbol{\omega})}{\partial \boldsymbol{\omega} \partial \boldsymbol{\omega}^T} \\
&= \begin{bmatrix} I_{11} & I_{12} & I_{13} \\ I_{21} & I_{22} & I_{23} \\ I_{31} & I_{32} & I_{33} \end{bmatrix} \\
&= E\begin{bmatrix} -\frac{\partial^2 \ln L(\boldsymbol{x}, \boldsymbol{\omega})}{\partial \alpha^2} & -\frac{\partial^2 \ln L(\boldsymbol{x}, \boldsymbol{\omega})}{\partial \alpha \partial \theta} & -\frac{\partial^2 \ln L(\boldsymbol{x}, \boldsymbol{\omega})}{\partial \alpha \partial \tau} \\ -\frac{\partial^2 \ln L(\boldsymbol{x}, \boldsymbol{\omega})}{\partial \theta \partial \alpha} & -\frac{\partial^2 \ln L(\boldsymbol{x}, \boldsymbol{\omega})}{\partial \theta^2} & -\frac{\partial^2 \ln L(\boldsymbol{x}, \boldsymbol{\omega})}{\partial \theta \partial \tau} \\ -\frac{\partial^2 \ln L(\boldsymbol{x}, \boldsymbol{\omega})}{\partial \tau \partial \alpha} & -\frac{\partial^2 \ln L(\boldsymbol{x}, \boldsymbol{\omega})}{\partial \tau \partial \theta} & -\frac{\partial^2 \ln L(\boldsymbol{x}, \boldsymbol{\omega})}{\partial \tau^2} \end{bmatrix},
\end{aligned}
$$

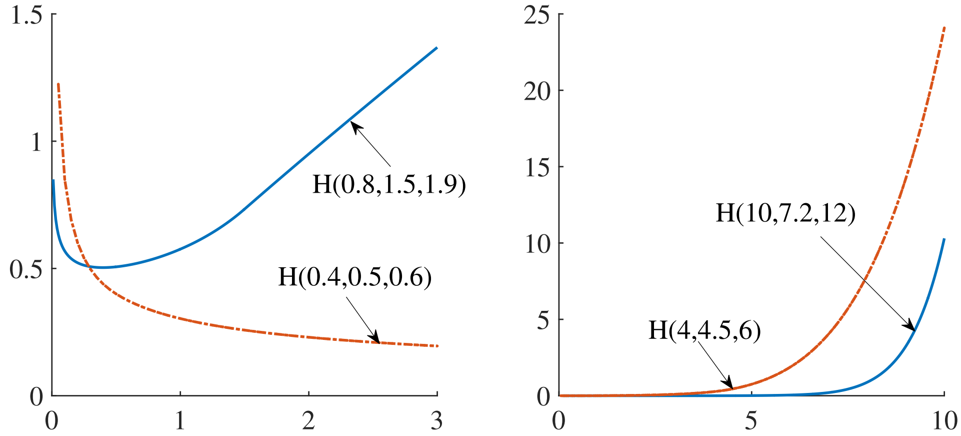


Fig 4. Plots of hazard rate functions of PFWC distribution

where the elements of the matrix are defined as:

$$I_{11} = \left[m + (n-2m)\frac{\alpha}{\tau}\right]\left[\frac{1}{\alpha^2} + \frac{1}{(\tau-\alpha)^2}\right],$$

$$\begin{aligned}I_{12} &= I_{21}\\ &= \frac{1}{\theta}\left[(n-m) + (3m-2n)\frac{\alpha}{\tau}\right]\\ &+ \frac{1}{\theta}(n-m)\frac{\alpha}{\tau}\frac{1}{1-\alpha/\tau}\left(2-\frac{\alpha}{\tau}\right),\end{aligned}$$

$$\begin{aligned}I_{13} &= I_{31}\\ &= -\frac{m}{\tau^2(1-\alpha/\tau)}\\ &- \frac{(n-m)\alpha}{\tau^3}\left[\frac{1}{(1-\alpha/\tau)^2} - b_1\left(1-\frac{\alpha}{\tau}\right)\exp\left(1-\frac{\alpha}{\tau}\right)\right],\\ I_{22} &= \frac{\alpha}{\theta^2}\left\{m\left(1-\frac{\alpha}{\tau}\right) - (n-m)\left[1-(\tau+1)\left(2-\frac{\alpha}{\tau}\right)\right]\right\}\\ &+ \frac{\alpha}{\theta^2}\left\{(2m-n)(\alpha+1)\left(1-\frac{\alpha}{\tau}\right)\right\},\end{aligned}$$

$$\begin{aligned}I_{23} &= I_{32} = -\frac{\alpha}{\theta\tau}(n-m)\frac{1}{(1-\alpha/\tau)}\\ &- \frac{\alpha}{\theta\tau}\left\{(n-m)b_1\left(1-\frac{\alpha}{\tau}\right)^2\exp\left(1-\frac{\alpha}{\tau}\right) + (2m-n)\frac{\alpha}{\tau}\right\}\\ I_{33} &= m\left(1-\frac{\alpha}{\tau}\right)\left[\frac{1}{(\tau-\alpha)^2} - \frac{1}{\tau^2}\right]\\ &+ \frac{(n-m)\alpha}{\tau^3}\left[\frac{2}{(1-\alpha/\tau)} + \frac{\alpha}{\tau(1-\alpha/\tau)^2} + 2\right]\\ &- \frac{2(n-m)\alpha^2}{\tau^3}\frac{1}{(\tau-\alpha)}\left(2-\frac{\alpha}{\tau}\right)\\ &+ \frac{(n-m)\alpha}{\tau^3}\left[\frac{2\alpha}{\tau}\exp\left(1-\frac{\alpha}{\tau}\right)b_1\right]\\ &+ \frac{(n-m)\alpha}{\tau^3}\left(1-\frac{\alpha}{\tau}\right)^2\exp\left(1-\frac{\alpha}{\tau}\right)b_2,\end{aligned}$$

where $b_1 = \int_1^{+\infty} u\ln u\exp(-(1-\alpha/\tau)u)\,\mathrm{d}u$ and $b_2 = \int_1^{+\infty} u(\ln u)^2\exp(-(1-\alpha/\tau)u)\,\mathrm{d}u$.

### B. Method of Moments

The method of moments (MM) is a parameter estimation technique that matches sample moments to the theoretical moments of a distribution. In the case of the PFWC distribution, the $r$th raw moment can be expressed as

$$E(X^r) = \theta^r\left[\frac{w\alpha}{(\alpha+r)} + \frac{\alpha}{\tau}e^w w^{-r/\tau} iga\left(1+\frac{r}{\tau}, w\right)\right], \tag{13}$$

where $iga(b,x) = \int_x^{+\infty} t^{b-1}\exp(-t)\,\mathrm{d}t$ is the upper incomplete gamma function.

From (13), the first, second, and third raw moments can be readily derived. Using the method of moments, the theoretical moments $\mathrm{E}(X)$, $\mathrm{E}(X^2)$, and $\mathrm{E}(X^3)$ are equated to their corresponding sample moments:

$$\frac{1}{n}\sum_{i=1}^n x_i, \frac{1}{n}\sum_{i=1}^n x_i^2, \text{ and } \frac{1}{n}\sum_{i=1}^n x_i^3,$$

respectively. This leads to the following nonlinear system of equations:

$$\begin{cases}\theta\left[\frac{w\alpha}{(\alpha+1)} + \frac{\alpha}{\tau}e^w w^{-1/\tau} iga\left(1+\frac{1}{\tau}, w\right)\right] = \frac{1}{n}\sum_{i=1}^n x_i,\\ \theta^2\left[\frac{w\alpha}{(\alpha+2)} + \frac{\alpha}{\tau}e^w w^{-2/\tau} iga\left(1+\frac{2}{\tau}, w\right)\right] = \frac{1}{n}\sum_{i=1}^n x_i^2,\\ \theta^3\left[\frac{w\alpha}{(\alpha+3)} + \frac{\alpha}{\tau}e^w w^{-3/\tau} iga\left(1+\frac{3}{\tau}, w\right)\right] = \frac{1}{n}\sum_{i=1}^n x_i^3.\end{cases} \tag{14}$$

This system can be solved iteratively for the parameters $(\alpha, \theta, \tau)$, yielding the method of moments estimators (MMEs) denoted by $\hat{\alpha}_{mm}, \hat{\theta}_{mm}$, and $\hat{\tau}_{mm}$.

### C. Nonlinear Least Squares Estimation

Nonlinear least squares (NLS) is a frequently employed technique for parameter estimation, which minimizes the difference between the empirical CDF and the order statistics. By applying the logarithm to Equation (7), we derive

$$\begin{cases}\ln F(x) = \ln w + \alpha\ln x - \alpha\ln\theta, \quad 0 < x \le \theta,\\ \ln(1-F(x)) = \ln w - w\left(\frac{x}{\theta}\right)^\tau, \quad \theta \le x < \infty.\end{cases} \tag{15}$$

In this method, it is necessary to use a plotting position to estimate the distribution function corresponding to the $i^{th}$

Table I: Biases and MSEs of MLEs for PFWC distribution

| $n$ | bias($\alpha$) | mse($\alpha$) | bias($\theta$) | mse($\theta$) | bias($\tau$) | mse($\tau$) |
|---|---|---|---|---|---|---|
| PFWC(2,5,2.5) | | | | | | |
| 10 | 0.1985 | 0.4748 | 3.1525 | 22.5913 | 12.0121 | 48.2889 |
| 20 | 0.0896 | 0.2330 | 1.8317 | 17.9147 | 7.6881 | 27.7242 |
| 50 | 0.1018 | 0.1480 | 0.2513 | 8.4966 | 6.2671 | 15.1875 |
| 100 | 0.0800 | 0.0834 | -0.1734 | 3.6947 | 1.9627 | 5.8948 |
| 200 | 0.0404 | 0.0353 | -0.1276 | 1.6047 | 0.0725 | 0.1464 |
| 500 | 0.0163 | 0.0108 | -0.0080 | 0.4509 | 0.0359 | 0.0421 |
| PFWC(10,8,15) | | | | | | |
| 10 | 1.2506 | 21.2075 | 0.4167 | 0.9731 | 17.9478 | 28.7112 |
| 20 | 0.9093 | 12.5836 | 0.1137 | 0.9228 | 5.5221 | 12.2384 |
| 50 | 0.5432 | 5.7755 | -0.1758 | 0.8717 | 3.8611 | 8.4252 |
| 100 | 0.4429 | 3.3993 | -0.2069 | 0.6396 | 1.1113 | 3.3361 |
| 200 | 0.2476 | 1.8073 | -0.1262 | 0.4000 | 0.5481 | 3.7932 |
| 500 | 0.0854 | 0.5547 | -0.0236 | 0.0768 | 0.2197 | 1.2715 |

Table II: Biases and MSEs of MMs for PFWC distribution

| $n$ | bias($\alpha$) | mse($\alpha$) | bias($\theta$) | mse($\theta$) | bias($\tau$) | mse($\tau$) |
|---|---|---|---|---|---|---|
| PFWC(2,5,2.5) | | | | | | |
| 10 | 0.0529 | 0.3177 | 0.0725 | 11.4781 | 2.6633 | 37.6517 |
| 20 | 0.0479 | 0.1556 | -0.1232 | 8.8290 | 1.7714 | 22.9067 |
| 50 | 0.0025 | 0.0690 | -0.1179 | 4.8208 | 0.5411 | 7.4750 |
| 100 | 0.0211 | 0.0428 | -0.1300 | 2.6565 | 0.1383 | 0.4718 |
| 200 | 0.0239 | 0.0276 | -0.0742 | 1.2185 | 0.0599 | 0.1198 |
| 500 | 0.0111 | 0.0108 | -0.0326 | 0.4436 | 0.0235 | 0.0419 |
| PFWC(10,8,15) | | | | | | |
| 10 | 2.2955 | 17.0902 | -0.4401 | 0.6524 | 14.0902 | 51.7285 |
| 20 | 1.2524 | 7.7237 | -0.3311 | 0.5463 | 7.0401 | 29.3602 |
| 50 | 0.7444 | 3.8830 | -0.2159 | 0.4115 | 4.0915 | 8.8716 |
| 100 | 0.4492 | 2.5312 | -0.1128 | 0.3322 | 4.4460 | 12.8579 |
| 200 | 0.2712 | 1.3561 | -0.0733 | 0.2137 | 2.9724 | 12.2004 |
| 500 | 0.1540 | 0.7101 | -0.0304 | 0.1251 | 1.6525 | 5.3423 |

order statistic. We take this as $p_i = \frac{i}{n+1}$. The nonlinear least squares estimators (NLSEs) of $\alpha$, $\theta$, and $\tau$, denoted by $\hat{\alpha}_{nls}$, $\hat{\theta}_{nls}$, and $\hat{\tau}_{nls}$, respectively, can be obtained by minimizing

$$G(\alpha,\theta,\tau) = \sum_{i=1}^{m} \{\ln p_i - \ln w - \alpha \ln x_i + \alpha \ln \theta\}^2 + \sum_{i=m+1}^{n} \left\{\ln(1-p_i) - \ln w + w\left[\left(\frac{x_i}{\theta}\right)^{\tau} - 1\right]\right\}^2, \tag{16}$$

which is solved similarly to (12).

### D. Simulation study

We present a Monte Carlo simulation to illustrate the estimation methods for PFWC(1.5,5,2.5) and PFWC(10,8,15), as described above. We note that PFWC(1.5,5,2.5) is right-skewed, with skewness coefficient of 0.2880, and PFWC(10,8,15) is left-skewed, with skewness coefficient of –1.0902.

We compare the performance of the MLEs, MMEs, and NLSEs in terms of biases and mean square errors (MSEs) using 10,000 replications, examining sample sizes ranging from very small ($n = 10$) to very large ($n = 500$). All computations were performed using MATLAB R2015b. Simulation study results are summarized in Tables I–III, from which we observe the following:

(1) As the sample size $n$ increases, the biases and mean squared errors (MSEs) generally decrease;

(2) For the PFWC(10,8,15) distribution, maximum likelihood estimators (MLEs) tend to have smaller biases and MSEs than method of moments estimators (MMEs), whereas for PFWC(1.5,5,2.5), MMEs typically outperform MLEs. This suggests no clear superiority between MLEs and MMEs;

(3) MMEs generally demonstrate better performance than nonlinear least squares estimators (NLSEs) in terms of both biases and MSEs.

Therefore, we recommend MLEs or MMEs for estimating the parameters of the PFWC distribution, with NLSEs as a secondary option.

## IV. Probability plot

The probability plot is a straightforward tool for evaluating whether a proposed distribution fits a given dataset. When the quantiles of the theoretical distribution are plotted against the sample order statistics, the points should approximately form a straight line if the distribution is a good fit. For the PFWC distribution, the quantile function is given by (8), and applying the logarithm to this function results in

Table III: Biases and MSEs of NLSEs for PFWC distribution

| $n$ | bias($\alpha$) | mse($\alpha$) | bias($\theta$) | mse($\theta$) | bias($\tau$) | mse($\tau$) |
|---|---|---|---|---|---|---|
| PFWC(2,5,2.5) | | | | | | |
| 10 | -0.0745 | 0.2653 | -0.0109 | 13.4437 | 2.2494 | 35.7349 |
| 20 | -0.0121 | 0.2285 | 0.0684 | 15.4717 | 3.6940 | 25.4868 |
| 50 | 0.0000 | 0.1673 | 0.0857 | 16.7614 | 4.4048 | 12.4749 |
| 100 | 0.0570 | 0.1425 | -0.6006 | 12.3572 | 1.5842 | 20.2862 |
| 200 | 0.0915 | 0.1095 | -1.0095 | 7.4364 | 0.4017 | 2.2671 |
| 500 | 0.0529 | 0.0604 | -0.5736 | 3.2979 | -0.0451 | 0.0682 |
| PFWC(10,8,15) | | | | | | |
| 10 | -0.8449 | 15.3496 | 0.0728 | 0.8581 | 14.3688 | 79.8894 |
| 20 | -0.5935 | 9.4413 | -0.0964 | 1.2272 | 23.8231 | 59.2279 |
| 50 | -0.1983 | 6.6545 | -0.4578 | 1.7664 | 4.6022 | 41.6809 |
| 100 | 0.3238 | 5.4045 | -0.7251 | 2.0540 | 3.7528 | 15.8347 |
| 200 | 0.5512 | 4.3639 | -0.7871 | 2.1494 | 1.4216 | 5.0974 |
| 500 | 0.4751 | 2.7880 | -0.6047 | 1.7755 | -0.2834 | 2.1547 |

$$\ln x(p) = \begin{cases} \ln\theta + \dfrac{1}{\alpha}\left(\ln p - \ln w\right), & 0 < p \le w, \\ \ln\theta + \dfrac{1}{\tau}\ln\left[1 - \dfrac{1}{w}\ln\left(\dfrac{1-p}{1-w}\right)\right], & w \le p < 1, \end{cases} \tag{17}$$

where $w = 1 - \alpha/\tau$. Define

$$p_1 = \begin{cases} \dfrac{1}{\alpha}\left(\ln p - \ln w\right), & 0 < p \le w, \\ \dfrac{1}{\tau}\ln\left[1 - \dfrac{1}{w}\ln\left(\dfrac{1-p}{1-w}\right)\right], & w \le p < 1. \end{cases} \tag{18}$$

Equation (18) can be rewritten as:

$$\begin{cases} \dfrac{1}{\alpha}\left(\ln p - \ln w\right) = -\ln\theta + \ln x, & 0 < x \le \theta, \\ \dfrac{1}{\tau}\ln\left[1 - \dfrac{1}{w}\ln\left(\dfrac{1-p}{1-w}\right)\right] = -\ln\theta + \ln x, & x \ge \theta. \end{cases} \tag{19}$$

Equation (19) describes a linear relationship between $p_1$ and $\ln x$, with an intercept of $-\ln\theta$ and a slope of 1. It is also evident that when $p = w$, $p_1 = 0$ and $x = \theta$. Figure 5 displays the probability plot for 100 sets of simulated data generated from the PFWC(10,8,15) distribution, using a random seed of 1234. The solid line AB in Figure 5 represents the probability plot constructed based on Equation (17). The starting point A and endpoint B correspond to the natural logarithms of the minimum and maximum values of the simulated data, denoted by $\ln(x_{min})$ and $\ln(x_{max})$, respectively. In this example, $\ln(x_{min}) = 1.7570$ and $\ln(x_{max}) = 2.2480$. The point $E(\ln\theta, 0)$ is the intersection of the lines $\ln x = \ln\theta$ and $p_1 = 0$, which precisely corresponds to $p = w = 1-\alpha/\tau = 1-10/15 = 0.3333$. The line $p_1 = 0$ divides AB into two segments. For the upper segment, AE, $p_1$ is $1/\alpha\,(\ln p - \ln w)$, while for the lower segment, BE, it is $\frac{1}{\tau}\ln\left[1-\frac{1}{w}\ln\left(\frac{1-p}{1-w}\right)\right]$. Additionally, the straight line $p = 0.3333$ divides AB into two regions: $p < 0.3333$ and $p > 0.3333$.

To assess whether the PFWC distribution is suitable for fitting a given dataset, we use a probability plot constructed as follows:

(1) Arrange the data in ascending order, denoted as $x = (x_1, x_2, \cdots, x_n)$;

(2) Obtain the maximum likelihood estimates (MLEs) of $\alpha$, $\theta$, and $\tau$, denoted as $\hat{\alpha}$, $\hat{\theta}$, and $\hat{\tau}$, respectively. Then compute $\hat{w} = 1-\hat{\alpha}/\hat{\tau}$;

(3) Compute $p_i = \dfrac{i}{n+1}$ for $i = 1, 2, \cdots, n$;

(4) Compute $\hat{p}_1$ from (19): $\hat{p}_{1i} = 1/\alpha\,(\ln p_i - \ln\hat{w})$ when $p_i < \hat{w}$, and $\hat{p}_{1i} = \frac{1}{\hat{\tau}}\ln\left[1-\frac{1}{\hat{w}}\ln\left(\frac{1-p_i}{1-\hat{w}}\right)\right]$ when $p_i > \hat{w}$;

(5) Plot $\hat{p}_1$ against $\ln x$. If the points approximately form a straight line, the PFWC distribution can be used to model the dataset.

## V. Goodness-of-fit tests

### A. The test statistics

Let $x = (x_1, x_2, \cdots, x_n)$ be an independent random sample drawn from a continuous distribution $F(x)$. In this study, a goodness-of-test is employedd to evaluate the null hypothesis:

$$H_0 : F(x) = F_0(x; \hat{\boldsymbol{\omega}}), \tag{20}$$

where $F_0(x;\hat{\boldsymbol{\omega}})$ represents the PFWC distribution with estimated parameters, $\hat{\boldsymbol{\omega}} = (\hat{\alpha}, \hat{\theta}, \hat{\tau})^T$. To assess whether the PFWC distribution is suitable for a given dataset, the following three goodness-of-fit tests are utilized:

- Kolmogorov–Smirnov ($D$):

$$D = \max_{0\le i\le n}\left\{max(D_1, D_2)\right\}, \tag{21}$$

where $D_1 = \dfrac{i}{n} - F_0(x_{(i)}, \hat{\boldsymbol{\omega}})$ and $D_2 = F_0(x_{(i)}, \hat{\boldsymbol{\omega}}) - \dfrac{i-1}{n}$. Here, $F_0(x_{(i)}, \hat{\boldsymbol{\omega}})$ is the estimated cumulative distribution function of the original sample.

- Anderson–Darling ($A^2$):

$$A^2 = -\frac{1}{n}\left\{\sum_{i=1}^{n}(2i-1)(A_1 + A_2)\right\} - n, \tag{22}$$

where $A_1 = \log\left[F_0(x_{(i)}, \hat{\boldsymbol{\omega}})\right]$, and $A_2 = \log\left[1 - F_0(x_{(i)}, \hat{\boldsymbol{\omega}})\right]$.

- Cramér–von Mises ($W^2$):

$$W^2 = \sum_{i=1}^{n}\left\{F_0(x_{(i)}, \hat{\boldsymbol{\omega}}) - \frac{i-0.5}{n}\right\}^2 + \frac{1}{12n}. \tag{23}$$

The Kolmogorov–Smirnov ($D$), Anderson–Darling ($A^2$), and Cramér–von Mises ($W^2$) tests are among the most widely used methods for assessing the goodness-of-fit of a null hypothetical distribution to data. For further details on these tests, refer to [19].

### B. Critical values of the test statistics

Suppose $x$ is a random variable following the PFWC distribution. Then, the transformed variable $y = w(x/\theta)^\alpha$ follows the distribution:

$$F(y) = \begin{cases} y, & 0 < y \le w, \\ 1-(1-w) & \\ \exp\left\{-w\left(\left(\dfrac{y}{w}\right)^{\dfrac{1}{1-w}} - 1\right)\right\}, & w \le y < \infty, \end{cases} \tag{24}$$

where $w = 1 - \alpha/\tau$. This transformation reduces the problem in (20) to testing whether the values of $y$ follow the distribution given in (24). Consequently, the null hypothesis becomes:

$$H_0 : F(y) = F_0(y; \hat{w}). \tag{25}$$

Since goodness-of-fit tests are not distribution-free when the population parameters must be estimated, different critical values correspond to different null hypotheses. In this case, both $y$ and the critical values of these tests depend solely on the value of $w$. Therefore, the Monte Carlo simulation technique is employed to determine the critical values for these tests for a given $w$. The procedure for finding the critical values of the $D$ test is as follows:

(1) Generate a random sample of size $n$ from the distribution (24) for a given $w$;

(2) Sort the data in ascending order, compute $F_0(y_{(i)}, w)$, and calculate $D$ using Equation (21);

(3) Repeat steps 1 and 2 20,000 times. Order the resulting 20,000 test statistics and determine the 80th, 85th, 90th, 95th, and 99th percentiles. These quantiles approximate the critical values for significance levels of 0.20, 0.15, 0.10, 0.05, and 0.01, respectively.

For $w = 0.4$, the critical values of the $D$, $A^2$, and $W^2$ tests are presented in Table IV for significance leves of 0.20, 0.15, 0.10, 0.05 and 0.01. For instance, when $n = 20$, the null hypothesis is rejected if the test statistic $D$ exceeds 0.2642, 0.2934, or 0.3523 at significance leves of 0.10, 0.05, and 0.01, respectively.

When the critical values of $D$ in table IV are compared with those in the standard table for the Kolmogorov-Smirnov test (Table 1 of [20]), it is evident that the Monte Carlo critical values closely align with the results of [20]. For instance, at a significance level of 0.05, the critical value of $D$ for $n = 20$ is 0.2935, which is very close to the value of 0.294 reported in [20]. Regarding the Anderson–Darling test, [21] provides a table of asymptotic significance points

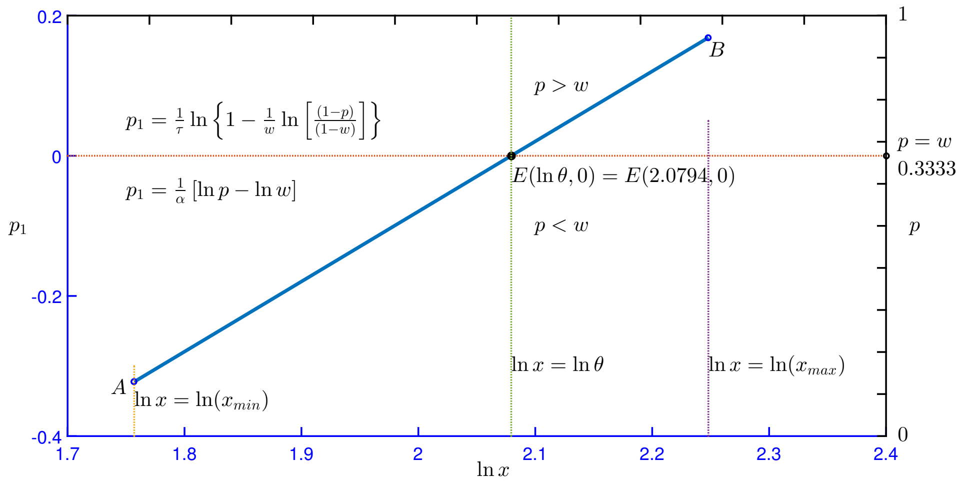


Fig 5. Probability plot for 100 sets of simulated PFWC(10,8,15) data

Table IV: Critical values for $D$, $A^2$, and $W^2$

| $n$ | Statistic | 0.20 | 0.15 | 0.10 | 0.05 | 0.01 |
|---|---|---|---|---|---|---|
| 5 | $D$ | 0.4446 | 0.4725 | 0.5080 | 0.5609 | 0.6629 |
| | $A^2$ | 1.3982 | 1.5995 | 1.9513 | 2.5044 | 3.9151 |
| | $W^2$ | 0.2407 | 0.2835 | 0.3375 | 0.4406 | 0.6791 |
| 10 | $D$ | 0.3224 | 0.3419 | 0.3679 | 0.4082 | 0.4817 |
| | $A^2$ | 1.4177 | 1.6281 | 1.9388 | 2.4914 | 3.7799 |
| | $W^2$ | 0.2414 | 0.2829 | 0.3448 | 0.4473 | 0.6904 |
| 20 | $D$ | 0.2314 | 0.2461 | 0.2642 | 0.2934 | 0.3523 |
| | $A^2$ | 1.4055 | 1.6137 | 1.9305 | 2.5035 | 3.9485 |
| | $W^2$ | 0.2415 | 0.2833 | 0.3464 | 0.4579 | 0.7362 |
| 40 | $D$ | 0.1662 | 0.1763 | 0.1891 | 0.2100 | 0.2522 |
| | $A^2$ | 1.4191 | 1.6318 | 1.9459 | 2.5503 | 3.9926 |
| | $W^2$ | 0.2434 | 0.2843 | 0.3477 | 0.4702 | 0.7471 |
| 60 | $D$ | 0.1361 | 0.1443 | 0.1557 | 0.1733 | 0.2062 |
| | $A^2$ | 1.4217 | 1.6288 | 1.9429 | 2.5163 | 3.8755 |
| | $W^2$ | 0.2445 | 0.2857 | 0.3485 | 0.4608 | 0.7459 |
| 80 | $D$ | 0.1180 | 0.1256 | 0.1351 | 0.1501 | 0.1789 |
| | $A^2$ | 1.4220 | 1.6371 | 1.9383 | 2.4951 | 3.8268 |
| | $W^2$ | 0.2443 | 0.2857 | 0.3486 | 0.4654 | 0.7221 |
| 100 | $D$ | 0.1053 | 0.1118 | 0.1206 | 0.1341 | 0.1606 |
| | $A^2$ | 1.4005 | 1.6083 | 1.9399 | 2.5260 | 3.8284 |
| | $W^2$ | 0.2387 | 0.2823 | 0.3456 | 0.4669 | 0.7263 |
| 200 | $D$ | 0.0751 | 0.0796 | 0.0856 | 0.0955 | 0.1141 |
| | $A^2$ | 1.4140 | 1.6253 | 1.9373 | 2.5073 | 3.8350 |
| | $W^2$ | 0.2420 | 0.2844 | 0.3500 | 0.4626 | 0.7336 |
| 400 | $D$ | 0.0533 | 0.0566 | 0.0608 | 0.0671 | 0.0803 |
| | $A^2$ | 1.4146 | 1.6343 | 1.9366 | 2.4981 | 3.7878 |
| | $W^2$ | 0.2437 | 0.2853 | 0.3479 | 0.4598 | 0.7238 |
| 600 | $D$ | 0.0434 | 0.0460 | 0.0497 | 0.0551 | 0.0658 |
| | $A^2$ | 1.4099 | 1.6123 | 1.9325 | 2.4909 | 3.8025 |
| | $W^2$ | 0.2418 | 0.2827 | 0.3492 | 0.4595 | 0.7257 |
| 800 | $D$ | 0.0376 | 0.0399 | 0.0430 | 0.0478 | 0.0566 |
| | $A^2$ | 1.4062 | 1.6232 | 1.9305 | 2.4886 | 3.8000 |
| | $W^2$ | 0.2413 | 0.2850 | 0.3464 | 0.4637 | 0.7293 |
| 1000 | $D$ | 0.0338 | 0.0358 | 0.0385 | 0.0427 | 0.0519 |
| | $A^2$ | 1.4238 | 1.6243 | 1.9332 | 2.4783 | 3.9608 |
| | $W^2$ | 0.2435 | 0.2872 | 0.3499 | 0.4556 | 0.7623 |

for $A^2$ at levels 0.10, 0.05, and 0.01, which are 1.933, 2.492, and 3.857, respectively. The values in Table IV show good agreement with these asymptotic values. For the Cramér–von Mises test, the asymptotic significance points for $W^2$ at levels 0.2, 0.15, 0.10, 0.05, and 0.01 are 0.2412, 0.2841, 0.3473, 0.4614, and 0.7435, respectively (Table 1 of [22]). Our results for $n = 1000$ are 0.2435, 0.2872, 0.3499, 0.4556, and 0.7623, respectively, demonstrating strong consistency with those of [22].

### C. Critical Value Approximations

To smooth the critical values in Table IV and facilitate future use of the test statistics, we modeled the critical values as functions of sample size. Specifically, we developed separate regression models for the critical values of the Kolmogorov–Smirnov ($D$) statistic at significance levels of 0.20, 0.15, 0.10, 0.05, and 0.01. The resulting models are as follows:

- $D_{0.20} = 0.004569 + \dfrac{1.003507}{\sqrt{n}}, (R^2 = 0.9993)$
- $D_{0.15} = 0.004799 + \dfrac{1.065908}{\sqrt{n}}, (R^2 = 0.9994)$
- $D_{0.10} = 0.005279 + \dfrac{1.146039}{\sqrt{n}}, (R^2 = 0.9993)$
- $D_{0.05} = 0.006258 + \dfrac{1.268593}{\sqrt{n}}, (R^2 = 0.9991)$
- $D_{0.01} = 0.009201 + \dfrac{1.501386}{\sqrt{n}}, (R^2 = 0.9986)$

Figure 6 displays the regression models (solid lines) alongside the tabled critical values for the $D$ test statistics (symbols) at significance levels of 0.20 and 0.01, showing excellent agreement. Additionally, the $R^2$ values of the regression models range from 0.9986 to 0.9994, indicating that the curves provide a strong fit to the tabled values. Similar graphs were also obtained for the remaining significance levels, further validating the accuracy of the models.

The critical values of the $A^2$ and $W^2$ statistics are plotted in Figures 7 and 8, respectively. It is evident that the critical values decrease as $\alpha$ increases for a fixed sample size $n$, while they remain relatively constant as $n$ increases for a fixed $\alpha$. Furthermore, Figures 7 and 8 reveal that the critical values of both statistics follow a similar pattern.

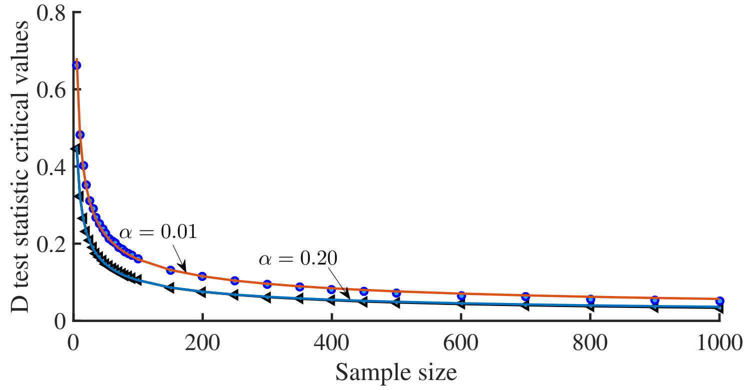


Fig 6. $D$ test statistic critival values

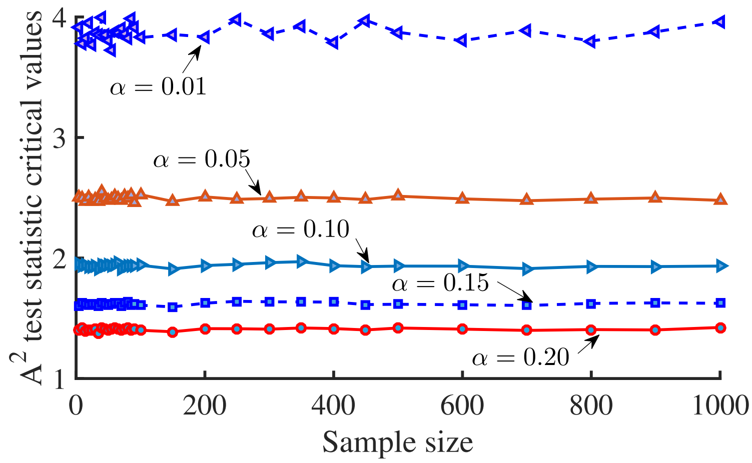


Fig 7. $A^2$ test statistic critival values

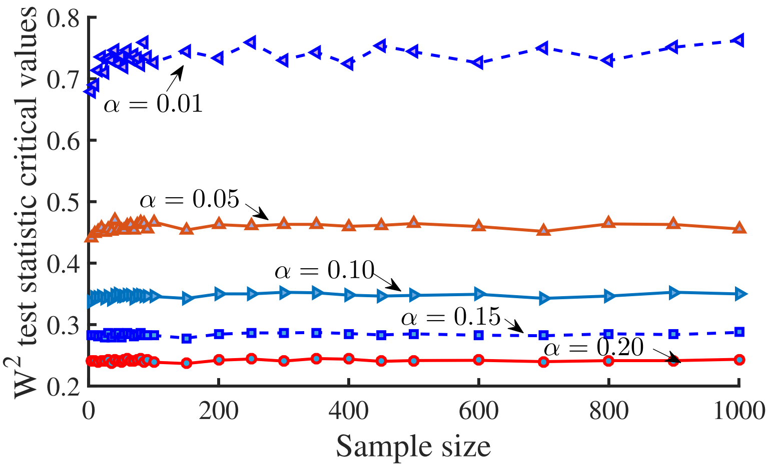


Fig 8. $W^2$ test statistic critival values

*D. Power comparison*

In statistics, the power of a test is defined as the probability of rejecting the assumed null hypothesis. In this subsection, we use the Monte Carlo approach to evaluate the power of the $D$, $A^2$, and $W^2$ tests for the PFWC distribution. Four alternative distributions are considered:

- Gamma(a,b): $\dfrac{1}{b^a\Gamma(a)}x^{a-1}e^{-x/b}$
- $\chi^2(v)$ : $\dfrac{x^{(v-2)/2}}{\Gamma(v/2)}2^{-v/2}e^{-x/2}$
- LN$(\mu,\sigma^2)$ : $\dfrac{1}{x\sigma\sqrt{2\pi}}\exp\left\{\dfrac{-(\ln x-\mu)^2}{2\sigma^2}\right\}$
- Weibull(a,b): $\dfrac{b}{a}\left(\dfrac{x}{a}\right)^{b-1}e^{-(x/a)^b}$

The null hypothesis is set as the PFWC(1.5,7,2.5) distribution, while the alternative distributions are Gamma(3.5,2.7), $\chi^2(10)$, LN(2.3,0.5), and Weibull(10,2). Figure 9 displays the density curves of these five competing distributions, showing that the differences between them are minimal.

The power of the tests was determined by generating 10,000 random samples of size $n$ from each of the four alternative distributions, with a significance level of 5%. The

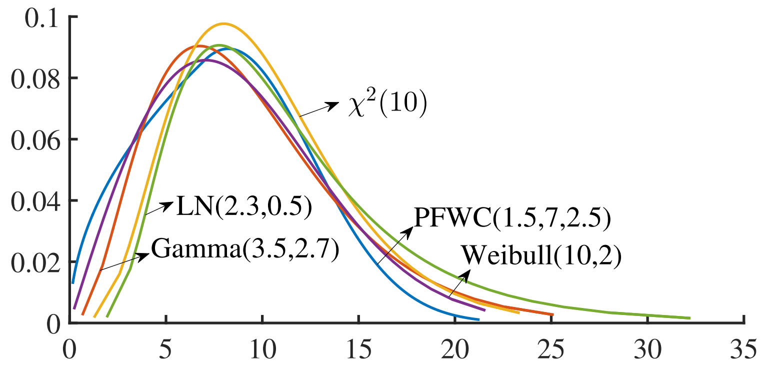


Fig 9. Density curves for PFWC(1.5,7,2.5) and four alternative distributions

Table V: Values of the power for testing the PFWC(1.5,7,2.5) for $D$, $A^2$, and $W^2$

| $n$ | Statistic | Gamma(3.5,2.7) | $\chi^2(10)$ | LN(2.3,0.5) | Weibull(10,2) |
|---|---|---|---|---|---|
| 10 | $D$ | 0.1921 | 0.0911 | 0.0702 | 0.2551 |
| | $A^2$ | 0.3073 | 0.1221 | 0.1007 | 0.4326 |
| | $W^2$ | 0.2099 | 0.1023 | 0.0723 | 0.2851 |
| 20 | $D$ | 0.3238 | 0.1148 | 0.0794 | 0.4313 |
| | $A^2$ | 0.4959 | 0.1683 | 0.1190 | 0.6664 |
| | $W^2$ | 0.3624 | 0.1370 | 0.0790 | 0.4846 |
| 40 | $D$ | 0.5493 | 0.1702 | 0.0843 | 0.6973 |
| | $A^2$ | 0.7385 | 0.2554 | 0.1288 | 0.8863 |
| | $W^2$ | 0.5877 | 0.2051 | 0.0815 | 0.7419 |
| 60 | $D$ | 0.7383 | 0.2521 | 0.0996 | 0.8745 |
| | $A^2$ | 0.8863 | 0.3662 | 0.1656 | 0.9747 |
| | $W^2$ | 0.7679 | 0.3012 | 0.0958 | 0.9062 |
| 80 | $D$ | 0.8574 | 0.3099 | 0.1118 | 0.9508 |
| | $A^2$ | 0.9530 | 0.4530 | 0.1945 | 0.9944 |
| | $W^2$ | 0.8760 | 0.3770 | 0.1037 | 0.9656 |
| 100 | $D$ | 0.9272 | 0.3826 | 0.1285 | 0.9828 |
| | $A^2$ | 0.9847 | 0.5420 | 0.2341 | 0.9990 |
| | $W^2$ | 0.9383 | 0.4526 | 0.1236 | 0.9866 |
| 150 | $D$ | 0.9877 | 0.5094 | 0.1638 | 0.9992 |
| | $A^2$ | 0.9984 | 0.7100 | 0.3190 | 1.0000 |
| | $W^2$ | 0.9902 | 0.6056 | 0.1565 | 0.9994 |
| 200 | $D$ | 0.9986 | 0.6527 | 0.2194 | 1.0000 |
| | $A^2$ | 0.9998 | 0.8381 | 0.4384 | 1.0000 |
| | $W^2$ | 0.9988 | 0.7463 | 0.2244 | 1.0000 |
| 400 | $D$ | 1.0000 | 0.9234 | 0.4324 | 1.0000 |
| | $A^2$ | 1.0000 | 0.9857 | 0.7755 | 1.0000 |
| | $W^2$ | 1.0000 | 0.9598 | 0.4733 | 1.0000 |
| 600 | $D$ | 1.0000 | 0.9873 | 0.6389 | 1.0000 |
| | $A^2$ | 1.0000 | 0.9993 | 0.9353 | 1.0000 |
| | $W^2$ | 1.0000 | 0.9951 | 0.6965 | 1.0000 |

results of the power study are summarized in Table V. Key observations from the comparison of the three tests include:

(1) For each test statistic, the power of rejection increases as the sample size $n$ increases;

(2) When the alternative distribution is LN(2.3,0.5), the power of all tests is the lowest, particularly for sample sizes smaller than 80, where the performance is extremly poor;

(3) For a fixed sample size $n$, the power of the tests decreases in the order $A^2$, $W^2$, and $D$. Thus, the $A^2$ test statistic demonstrates the highest power of rejection, outperforming both the $W^2$ and $D$ test statistics.

## VI. Data analysis

We analyze two datasets using the proposed distribution.

The first dataset (Example 3.4.1 of [3]) consists of the number of cycles to failure for 60 electrical appliances in a life test. [3] studied this dataset using nonparametric estimates of hazard rate functions. The 60 observations, sorted in ascending order, are as follows:

14, 34, 59, 61, 69, 80, 123, 142, 165, 210, 381, 464, 479, 556, 574, 839, 917, 969, 991, 1064, 1088, 1091, 1174, 1270, 1275, 1355, 1397, 1477, 1578, 1649, 1702, 1893, 1932, 2001, 2161, 2292, 2326, 2337, 2628, 2785, 2811, 2886, 2993, 3122, 3248, 3715, 3790, 3857, 3912, 4100, 4106, 4116, 4315, 4510, 4584, 5267, 5299, 5583, 6065, 9701.

The second dataset (Table 2.2 of [24]) consists of the service times (hours of operation without failure) of aircraft windshields at the time of observation. This dataset was analyzed by [23] using the Weibull distribution and by [15] using the Weibull-Lomax distribution. The 65 observations are as follows:

46, 140, 150, 248, 280, 313, 389, 487, 622, 900, 952, 996, 1003, 1010, 1085, 1092, 1152, 1183, 1244, 1249, 1262, 1360, 1436, 1492, 1580, 1719, 1794, 1915, 1920, 1963, 1978, 2053, 2065, 2117, 2137, 2141, 2163, 2183, 2240, 2341, 2435, 2464, 2543, 2560, 2592, 2600, 2670, 2717, 2819, 2820, 2878, 2950, 3003, 3102, 3304, 3483, 3500, 3622, 3665, 3695, 4015, 4628, 4806, 4881, 5140.

We denote the first and second datasets as LIFE and SERVICE, respectively. Their basic descriptive statistics are shown in Table VI. Both datasets exhibit positive skewness and are leptokurtic, which are typical characteristics of lifetime data. However, the log-transformed datasets, log(LIFE) and log(SERVICE), display left-skewness and leptokurtosis. This suggests that a left-skewed distribution, which is uncommon for lifetime data, would be required to model the log-transformed data. This feature is further illustrated in Figure 10, where the histograms of LIFE and SERVICE are heavily right-skewed, while their log-transformed counterparts are clearly left-skewed.

Table VII presents the maximum likelihood estimates (MLEs) of $\alpha$, $\theta$, and $\tau$, along with their corresponding asymptotic standard errors (in parentheses), derived from the associated Fisher information matrix.

To assess the goodness-of-fit of the PFWC distribution, we conducted the Kolmogorov–Smirnov ($D$), Anderson–Darling

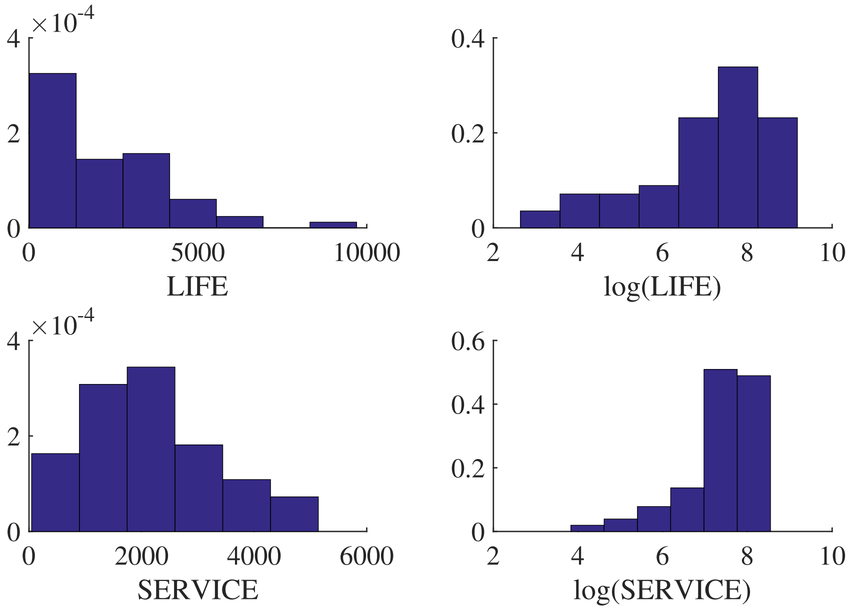


Fig 10. Histograms of data

Table VI: Descriptive statistics of LIFE and SERVICE data

| | LIFE | Log(LIFE) | SERVICE | Log(SERVICE) |
|---|---|---|---|---|
| Mean | 2193.03 | 7.0675 | 2081.42 | 7.3637 |
| Standard Error | 1920.15 | 1.4514 | 1230.39 | 0.9200 |
| Median | 1675.50 | 7.4237 | 2065.00 | 7.6329 |
| Minimum | 14.00 | 2.6391 | 46.00 | 3.8286 |
| Maximum | 9701.00 | 9.1800 | 5140.00 | 8.5448 |
| Skewness | 1.2613 | -1.1854 | 0.4485 | -1.6316 |
| Kurtosis | 5.2313 | 3.7356 | 2.7837 | 5.9128 |

Table VII: MLE of parameters (standard errors in parentheses)

| | $\hat{\alpha}$ | $\hat{\theta}$ | $\hat{\tau}$ |
|---|---|---|---|
| Log(LIFE) | 4.3481(0.8086) | 7.9676(0.1797) | 14.6985(2.3547) |
| Log(SERVICE) | 8.0592(1.7684) | 7.6578(0.1292) | 18.2512(2.3056) |

($A^2$), and Cramér–von Mises ($W^2$) tests for the cumulative distributions of the data under the PFWC hypothesis. Generally, smaller values of these test statistics indicate a better fit. The results, including the test statistics and p-values (in parentheses), are reported in Table VIII. These results demonstrate that the log-transformed LIFE and SERVICE datasets can be statistically well-described by the PFWC distribution.

Figure 11 shows the empirical survival function with 99% confidence bounds, along with the fitted PFWC distribution. Figure 12 presents the probability plot against the PFWC, as described in Section IV. From Figure 11, it is evident that the fitted PFWC distribution lies within the confidence bounds. Similarly, Figure 12 shows that the data points approximately follow a straight line. These graphical results suggest that the PFWC distribution is a suitable choice for modeling the two datasets.

Table VIII: EDF goodness-of-fit measures for fitted PFWC

| | $D$ | $W^2$ | $A^2$ |
|---|---|---|---|
| Log(LIFE) | 0.4306(0.6902) | 0.0684(0.5400) | 0.0917(0.6942) |
| Log(SERVICE) | 0.4209(0.6971) | 0.0677(0.5423) | 0.0867(0.7124) |

## VII. Conclusion

We introduced a three-parameter Power Function-Weibull Composite (PFWC) distribution and investigated its key properties, including the probability density function (PDF), cumulative distribution function (CDF), quantile function, survival function, and hazard rate function. We also discussed three estimation methods for the distribution parameters: maximum likelihood estimation (MLE), method of moments (MM), and nonlinear least squares (NLS). The performance of these methods was compared through extensive Monte Carlo simulations. Additionally, we computed the critical values of three goodness-of-fit test statistics—Kolmogorov–Smirnov ($D$), Anderson–Darling ($A^2$), and Cramér–von Mises ($W^2$)—using Monte Carlo simulations. The power of the proposed tests against four alternative distributions was also evaluated through Monte Carlo simulations. To demonstrate the practical utility of the PFWC distribution, we applied it to two real lifetime datasets. Unlike most studies, we found that the log-transformed lifetime data, rather than the original data, can be effectively modeled by the PFWC distribution, as confirmed by probability plots and goodness-of-fit tests. This finding provides a novel approach for modeling lifetime data.

## Acknowledgments

We thank LetPub (www.letpub.com.cn) for its linguistic assistance during the preparation of this manuscript.

## References

[1] J. D. Kalbfleisch and R. L. Prentice, *The Statistical Analysis of Failure Time Data*, 2nd ed. New York, NY, USA: John Wiley & Sons, 2011.

[2] W. B. Nelson, *Applied Life Data Analysis*, 2nd ed. New York, NY, USA: John Wiley & Sons, 2005.

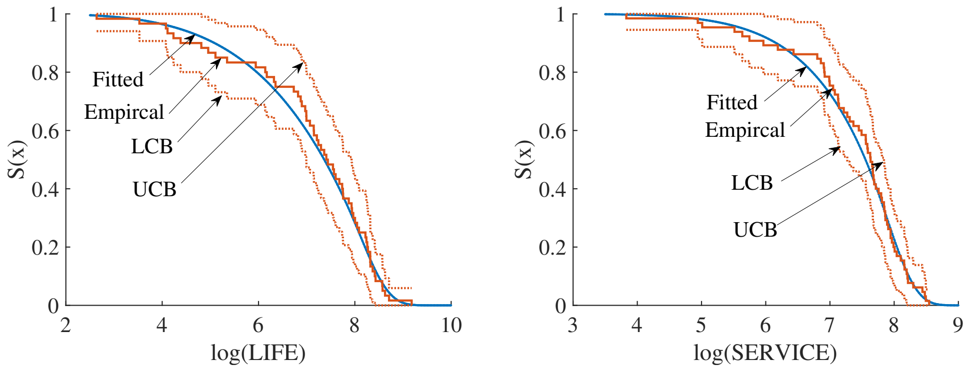


Fig 11. Survival estimates produced by Kaplan–Meier versus fitted PFWC distribution

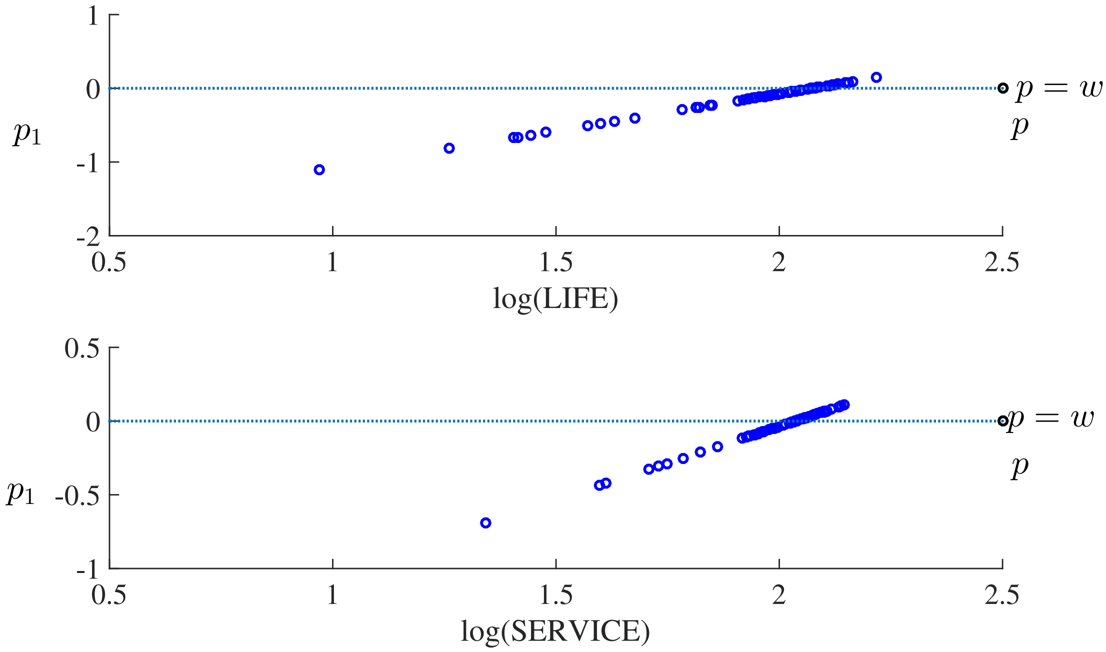


Fig 12. Probability plot against FPWC of data


[3] J. F. Lawless, *Statistical Models and Methods for Lifetime Data*. New York, NY, USA: John Wiley & Sons, 2003.

[4] W. Q. Meeker, L. A. Escobar, and F. G.Pascual, *Statistical Methods for Reliability Data*. New York, NY, USA: John Wiley & Sons, 1998.

[5] K. Cooray and M.M. A. Ananda, "Modeling actuarial data with a composite Lognormal–Pareto model," *Scandinavian Actuarial Journal*, vol. 2005, no. 5, pp. 321–334, 2005.

[6] D. P. M. Scollnik, "On composite lognormal-Pareto models," *Scandinavian Actuarial Journal*, vol. 2007, no. 1, pp. 20–33, 2007.

[7] S. Teodorescu and R. Vernic, "A composite Exponential–Pareto distribution," *The Annals of the "Ovidius" University of Constanta, Mathematics Series*, vol. XIV, no. 1, pp. 99–108, 2006.

[8] K. Cooray, "The Weibull–Pareto Composite Family with Applications to the Analysis of Unimodal Failure Rate Data," *Communication in Statistics-Theory and Methods*, vol. 38, no. 11, pp. 1901–1915, 2009.

[9] K. Cooray, S. Gunasekera and M.M. A. Ananda, "Weibull and inverse Weibull composite distribution for modeling reliability data," *Model Assisted Statistics and Applications*, vol. 5, no. 2, pp. 109–115, 2010.

[10] D. P. M. Scollnik and C. Sun, "Modeling with Weibull-Pareto Models," *North American Actuarial Journal*, vol. 16, no. 2, pp. 260–272, 2012.

[11] S. Nadarajah and S. A. A. Bakar, " New composite models for the Danish fire insurance data," *Scandinavian Actuarial Journal*, vol. 2014, no. 2, pp. 180–187, 2014.

[12] S. A. A. Bakar, N. A. Hamzaha, M. Maghsoudia, and S. Nadarajah, " Modeling loss data using composite models," *Insurance: Mathematics and Economics*, vol. 2015, no. 61, pp. 146–154, 2015.

[13] K. Cooray and C. I. Cheng, "Bayesian estimators of the lognormal–Pareto composite distribution," *Scandinavian Actuarial Journal*, vol. 2015, no. 6, pp. 500–515, 2015.

[14] E. Calderín-Ojeda, "On the Composite Weibull–Burr Model to describe claim data," *Communications in Statistics-Case Studies, Data Analysis and Applications*, vol. 1, no. 1, pp. 59–69, 2015.

[15] M. M. H. Tahir, G. M. Cordeiro, M. Mansoor, and M. Zubair, "The Weibull-Lomax distribution: Properties and Applications," *Hacettepe Journal of Mathematics and Statistics*, vol. 44, no. 2, pp. 461–480, 2015.

[16] E. Calderín-Ojeda, "The distribution of all French communes: A composite parametric approach," *Physica A: Statistical Mechanics and its Applications*, vol. 450, pp. 385–394, 2016.

[17] C. Wang, "The Power Function Lognormal Distribution: A New Probability Model for Insurance Claims Data," *Engineering Letters*, vol. 30, no. 1, pp. 1–8, 2022.

[18] C. Wang, "Parameter estimation for power function-lognormal composite distribution," *Communications in Statistics-Theory and Methods*, vol. 52, no. 9, pp. 2966–2982, 2023.

[19] R. B. D'Agostino and M. A. Stephens, *Goodness-of-fit techniques*, New York, NY, Marcel Dekker, 1986.

[20] F. J. Massey, "The Kolmogorov-Smirnov test for goodness of fit," *Journal of the American Statistical Association*, vol. 46, no. 253, pp. 68–78, 1951.

[21] T. W. Anderson and D. A. Darling, "A test of goodness of fit," *Journal of the American Statistical Association*, vol. 49, no. 268, pp. 765–769, 1954.

[22] T. W. Anderson and D. A. Darling, "Asymptotic theory of certain

goodness of fit criteria based on stochastic processes," *Annals of Mathematical Statistics*, vol. 23, no. 2, pp. 193–212, 1952.

[23] D. P. Murthy, *Weibull Models*. New York, NY, USA: John Wiley & Sons, 2004.

[24] W. R. Blischke and D. P. Murthy, *Reliability: Modeling, Prediction, and Optimization*. New York, NY, USA: John Wiley & Sons, 2011.